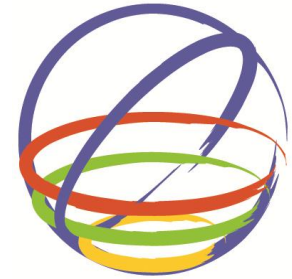


# Comparison of 2D vs. 3D Modeling Approaches for the Analyses of Concrete Faced Rockfill Dams



**15 WCEE**  
LISBOA 2012

**H. F. Özel & Y. Arici**

*Dept. of Civil Engineering, Structural Mechanics Laboratory, K2-303,  
Middle East Technical University, 06531, Turkey*

## **SUMMARY:**

This paper's primary purpose is to compare the 2 and 3D analysis methodologies for investigating the performance of a CFRD under dynamic loading conditions. The state of stress on the face plate is obtained in both cases using a total strain based crack model to predict the spreading of cracks on the plate and the corresponding crack widths. Results of the 2 and 3D analyses agree well. Although significantly more demanding, 3D analyses have the advantage of predicting 1) the opening of the vertical construction joints 2) the cracking at the valley sides 3) the crushing of the plate during the seismic action. During the earthquake loading, the cracking observed at the base of the face plate after the impounding spread significantly towards the crest of the dam; however the crackwidths were obtained relatively small. The openings at the construction joints were limited except in the maximum design earthquake condition.

*Keywords: CFRD, Earthquake, Interface, Crack, Face Plate*

## **1. INTRODUCTION**

Higher concrete faced rockfill dams (CFRDs) are being built all around the world due to the advantages of speed and ease of construction offered by this technology. Some very high CFRDs are also being built in countries with significant seismic risk such as China and Turkey. These systems are mostly designed based on precedent; the reduction in the face plate thickness and the reinforcement ratio is the major trend in the recent decades. However, the construction of higher CFRD dams, and their respective performance, led to the questioning of the common logic in the design of these systems. Significant cracking on the face plate led to significant leakage from the dam triggering drawdowns for some systems, pointing out to the need for advanced analysis for the prediction of CFRD performance (Sobrinho et al. 2007, Pinto, 2007, Johannesson & Tohlang, 2007, Chen & Han, 2009). In this regard, the main purpose of this study is to compare the 2D and 3D analysis models for predicting the performance of such systems. The cracking on the face plate, the separation of the slab at the vertical face and plinth joints and the crushing of the face plate are assumed as the design response parameters; prediction of these parameters with 2&3D finite element models, employing nonlinear material models calibrated to component testing, are investigated under the impoundment and earthquake loading.

## **2. THE COKAL CFRD**

The Cokal Dam, selected as the case study, is an 83-m-high CFRD with a crest length of 605 m that is being built for irrigation and flood prevention in northwest Turkey at the Thracian peninsula. The dam site is located less than 10 km from an extension of the North Anatolian Fault under the Marmara Sea. A typical cross-section of the dam is shown in Fig. 2.1.a. along with a selection of the materials that will be used at the site. The side slopes are 1H:1.4V, whereas the face plate is 50 cm thick. The reinforcement on the plate was assumed to correspond to 0.6% of the gross concrete area.

The Cokal Dam was modeled and analyzed in 2 and 3D configurations using the general purpose finite element software DIANA (TNO DIANA. 2009). A total of 4600 six-node isoparametric plane-strain triangular elements with a three-point integration scheme were used in modeling the rockfill, whereas 54 three-node infinite shell elements, with each node having two in plane and one rotational degree of freedom, were used to represent the face plate for the two 2D model. Embedded reinforcements, which do not have degrees of freedom of their own, are smeared in the face slab elements. The face plate elements were connected to the rockfill with line interface elements, based on quadratic interpolation. A nodal interface element was used at the bottom of the face plate to properly model any possible separation from the foundation at the plinth.

The embankment for the 3D model (Figure 2.1c) was comprised of 48000 10-node pyramid elements based on quadratic interpolation. A total of 4000 six-node iso-parametric curved shell elements were used to simulate the face plate with a similar reinforcement formulation as given in the 2D case. Vertical construction joints and the face plate-plinth base joints were modeled using 4000 line interfaces composed of 3+3 nodes. In order to model the interaction between the face plate and the rockfill, approximately 4000 plane interfaces in a 6+6 node configuration were utilized. The 3D model was roughly comprised of 200000 degrees of freedom. The Cokal Dam rests on medium-hard rock with a Young's modulus that is approximately two orders of magnitude greater than that of the fill material; therefore, the foundation of the dam was not included in the models, and the base was assumed to be a fixed support. Comparison of the 2 and 3D model results was conducted for the results obtained at the middle of the dam at a representative cross-section as given in Figure 2.1.

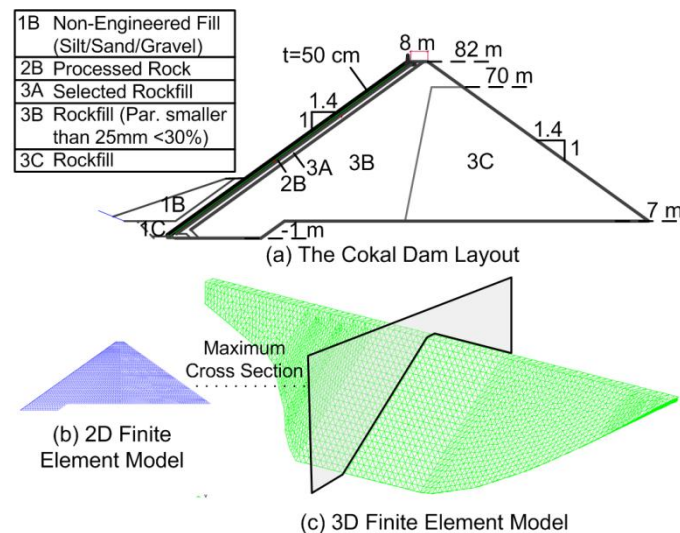


**Figure 2.1.** Cokal Dam Layout and the Finite Element Models

### 3. MATERIAL MODELING

The various constitutive models used in the analyses of the Cokal Dam are described in this section.

#### 3.1. Reinforced Concrete

The constitutive model used for concrete is based on the total strain rotating-crack model (Feenstra et al. 1989). The basic concept of the total strain crack models is that the stress is evaluated in the directions which are given by the crack directions. The compressive behavior was defined by a parabolic response, with  $f_c$  defining the peak strength. The crushing behavior and the ultimate strain are governed by the compressive fracture energy  $G_c$  so that the model is objective and mesh-independent. The tensile behavior was modeled by using a linear softening function beyond the tensile

strength  $f_t$ , with the ultimate tensile strain based on the tensile fracture energy  $G_f^I$ . A typical strain hardening diagram was chosen for the embedded reinforcement.

Crack widths for the cracks on the face plate were estimated using the empirically well-established Gergely-Lutz expression (Gergely & Lutz. 1968), which is commonly used in reinforced concrete design (ACI. 2004), relating the maximum crack width  $w_{\max}$  to three variables: the reinforcement steel strain at the crack ( $\varepsilon_{scr}$ ), the concrete cover over the reinforcement  $d_c$  and the area of concrete around each bar  $A$ :

$$w_{\max} = 2.2\beta_{GL}\varepsilon_{scr}\sqrt[3]{d_c A} \quad (3.1)$$

where  $\beta_{GL}$  is a factor that accounts for the strain gradient within the member.

### 3.2. Rockfill Constitutive Models

Triaxial experiments conducted on rockfill specimens reveal that (Varadarajan et al. 2003) the stress-strain behavior of rockfill material is nonlinear, inelastic and stress-dependent. A modified Mohr-Coulomb formulation (Groen. 1995), as implemented in (TNO DIANA. 2009), was used in this study to model the behavior of the rockfill under static loading including (1) the hardening with increasing shear stress, (2) the volumetric deformations and (3) the dependency of the mechanical properties on the confinement stress. This constitutive relationship utilizes nonlinear elasticity combined with a smooth, hardening shear yield surface and a circular-shaped compression cap. The simulation of the behavior of the fill during cyclic loading was conducted using a modified Ramberg-Osgood formulation. The stiffness degradation and the hysteretic damping of the rockfill material under cyclic strain is described in this model by Eqn. 3.2. and 3.3. The parameters  $\alpha$  and  $\beta$  that define the dynamic backbone function for this formulation are determined using the reference shear strain ( $\gamma_r$ ) and the maximum damping value ( $\xi_{\max}$ ).

$$\gamma_{xy} = \frac{\sigma_{xy}}{G} \left( 1 + \alpha |\tau_{xy}|^\beta \right) \quad (3.2)$$

$$\alpha = \left( \frac{2}{\gamma_r G} \right)^\beta \quad \& \quad \beta = \frac{2\pi\xi_{\max}}{2 - \pi\xi_{\max}} \quad (3.3)$$

$G = G_{ref} (p'/p_a)^{0.5}$  was assumed as the tangent shear modulus in the above formulation, defined by the current mean effective stress  $p'$ , the atmospheric pressure  $p_a$  and the reference shear modulus. The dependency of the damping ratio and stiffness degradation on the confining stress (Seed et al. 1984) at a given position in the rockfill was considered by defining the reference shear strain in Eqn. 3.2. as a function of the mean stress  $p'$  ( $\gamma_r = a \exp(bp')$ ) at that location. The details of this calibration are provided in Arici (2011).

### 3.3. Interface Modeling

Consistent with the findings of Zhang and Zhang (2009), the interface between the slab and the cushion layer was assumed to be governed by frictional behaviour simulated using a simple Mohr-Coulomb elasto-plastic model (Vermeer. & DeBorst. 1984). The interface element was calibrated to the test results given in Zhang and Zhang (2009), for a concrete-gravel layer contact. The behavior of the interfaces at the vertical construction joints of a CFRD (and at the plinth base) was simulated using

a Coulomb elasto-plastic model coupled with a gap criterion (TNO DIANA. 2009). When the tensile traction normal to the plane of the interface overcame the tensile strength of the concrete, a gap was assumed to form at the interface with an instant reduction in the normal stress (brittle behavior).

## 4. STATIC ANALYSIS FOR IMPOUNDING

### 4.1. Analysis Technique:

The settlement of the rockfill during the impounding stage is a loading condition on the face plate with the load transfer being controlled by the face-plate-cushion layer interface. Modeling of the loading stages of the plate is important to realistically predict the behavior of the face plate as the transfer is dependent on three different components acting in a non-linear fashion, i.e. the face plate concrete, the interface filler material and the rockfill. In order to represent the proper sequence of loading on the plate, the rockfill was built in 27 stages in 3m increments for the 2D model, after which, the reinforced concrete plate was created on the top of the rockfill connected to the plate with the interface elements. The impounding process was then modeled with the reservoir rising to the maximum water level (MWL) in 27 steps. The sequence of modeling for this case is presented in Figure 4.1a. For the 3D model, the fill is created in a single step, followed by the birth of the face plate on the top of the fill, later to be loaded incrementally with the reservoir rising similarly to the 2D model (Figure 4.1b). The face plate construction is going to happen independently of the building of the embankment of the Cokal Dam, implying that the face plate will rest on a fill that has gone through its static displacements. Hence, the stress state on the plate was obtained very similarly for both cases irrespective of the displacement obtained on the fill at the end of the construction stage.

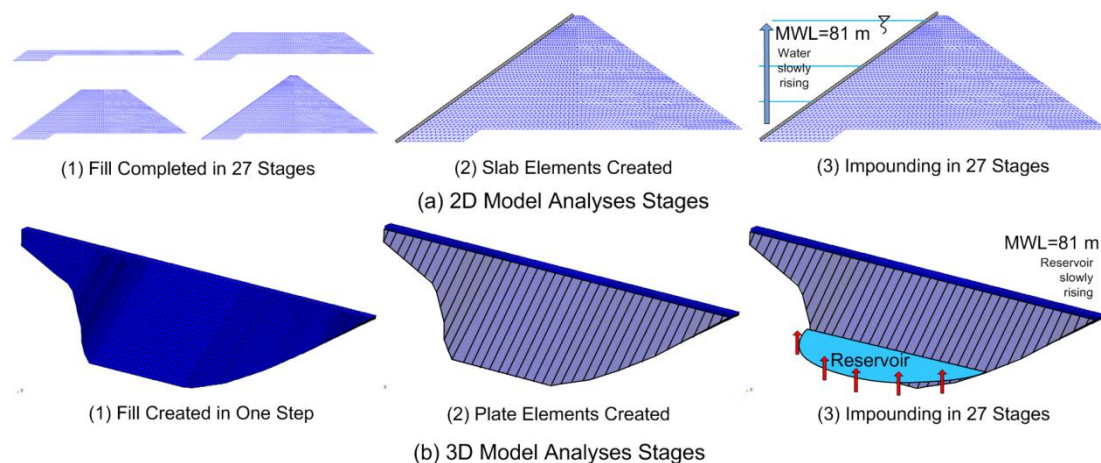


**Figure 4.1.** 2D and 3D Analysis Schemes Representing the Loading Stages

### 4.2. Comparison of the Results from 2 and 3D Models

The impounding of the reservoir changed the state of stress relatively significantly only near the upstream face of the dam. As given in Figure 4.2.a., the state of vertical stresses on the fill at the maximum cross-section was obtained very similarly for the 2 and 3D models. The vertical displacements obtained from the 2 and 3D models at the maximum cross section are compared in Figure 4.2.b. While the patterns of the fill displacement were similar for both models, the displacements obtained from the 3D analysis were smaller showing the effects of the valley sides on this response parameter.

The state of the stress on the face plate at the end of the impounding stage is provided in Figure 4.2.b. for the 2 and 3D models. The pattern of cracking on the face plate obtained from the two models agreed well, with the cracking spreading as much as 60m from the plinth base towards the crest of the dam. The 2D model reproduced the cracking behavior better due to the mesh density: the residual

stresses between the cracked elements of the face plate were obtained more clearly. The widths of the cracks on the face plate were obtained similarly for both models as well. The maximum crackwidth obtained for both models was around 0.5mm.

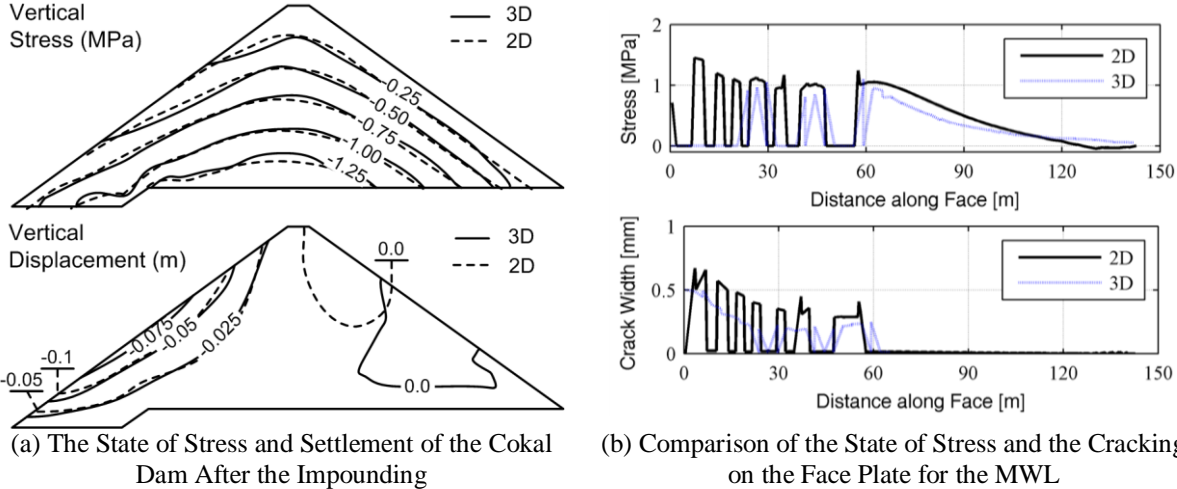


Figure 4.2. The Comparison of the Static Analyses Results

4.3. Spatial Effects of the Impounding on the Face Plate

The use of 2D analysis is not sufficient to represent some of the critical aspects of the behavior of a CFRD. The state of stress on the face plate near the valley boundaries, the behavior of the vertical construction joints (detailed with water stoppers), the performance of the lateral joints at the plinth base and the formation of inclined cracking (tensile and shear) on the face plate cannot be predicted in a 2D analysis. The change in the state of the stress on the face plate obtained by simulating this process with a 3D model is presented in Figure 4.3. The face slab was in a state of pure compression in the vertical direction (slope direction) initially with the stress increasing linearly towards the plinth base. The rising of the reservoir causes the stresses on the plate to slowly revert to tensile stresses. In the final stage, most of the face plate was in tension. The contour plot shown in Figure 4.3 displays a significant number of broken contour lines as a result of the cracking of the plate and the corresponding discontinuities in the plate stresses. A significant area of the face plate was in a cracked state at the end of the impounding of the dam, albeit with horizontal cracks of very small width running parallel to the dam axis.

The state of stress on the face plate parallel to the dam axis shows that there is very little stress on the plate in this direction after the construction stage (Figure 4.3.b.). As the reservoir level was raised, compressive stresses were observed on the submerged locations of the face plate. The raising of the reservoir led to an inner area of compression on the face plate surrounded by zones of tensile stress zones as one approaches the valley boundaries and the crest of the dam.

The nature of the cracking on the face plate as a result of this stress transfer is presented in Figure 4.4.a. The main form of cracking on the face plate after the impounding was in terms of horizontal cracks parallel to the dam axis, opening up in the up-down direction. Cracking was mainly concentrated at the base of the plate near the valley sides. Cracking in the vertical direction, also displayed in Figure 4.4.a., was very limited (crackwidths smaller than 0.1mm) and concentrated at the bottom of the boundaries of the face plate intersecting the valley sides.

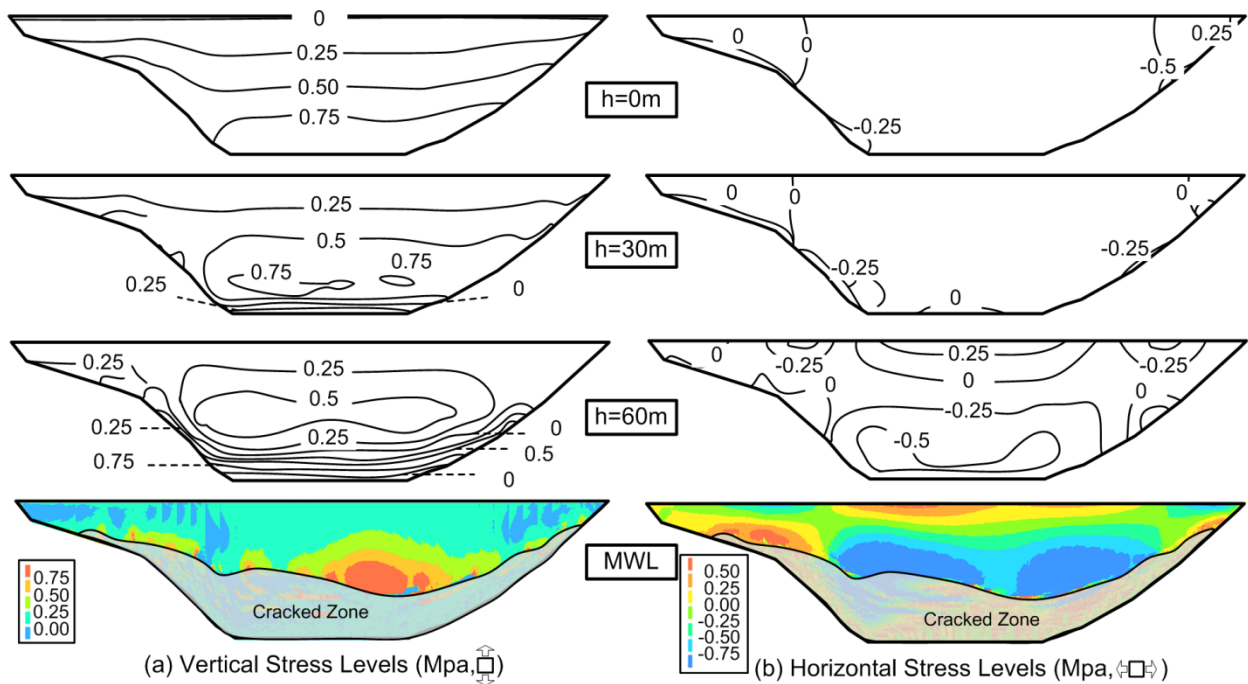


**Figure 4.3.** The State of Stress on the Face Plate

The specification of the vertical joints that will open up during the impounding process is usually deemed very important by the designers of such systems. For the Cokal Dam, the tensile strength of the vertical cold joints was not exceeded during the impounding stage. The distribution of the stresses on the vertical interfaces (normal to the interface plane) is presented in Figure 4.4.b. On the other hand, the tensile strength of the joints at the plinth base was exceeded leading to the separation at the interfaces at this location (Figure 4.4.c.). The maximum opening between the plinth base and the face plate was obtained to be around 0.5 cm from the 3D analysis, in contrast to the corresponding value of 0.8 cm obtained from the 2D study.

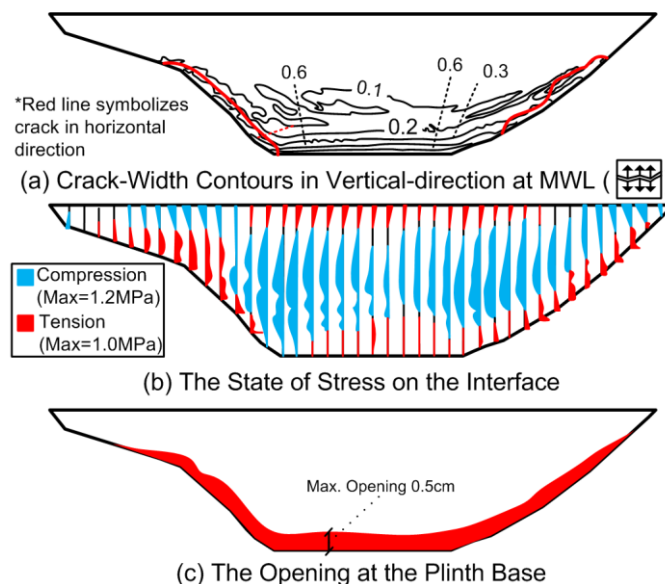


**Figure 4.4.** Contours of Crack Width at the Maximum Reservoir Level

## 5. THE EFFECT OF EARTHQUAKE LOADING ON THE COKAL DAM

### 5.1. Seismic Hazard Study

The Cokal Dam is located in a seismically critical region close to the active North Anatolian Fault. A site-specific seismic hazard study was conducted for the project in order to establish the design response spectra (Figure 5.1.a.) for the earthquake events with 144, 475, 975 and 2475 yr return periods. The OBE and the MDE events were chosen as the events with 144 and 2475 return periods, respectively. For the nonlinear transient time history analyses of the Cokal Dam, time histories that were response-spectrum matched to the target spectra were used. The ground motions developed for the 144, 475, 975 and 2475 year events are presented in Figure 5.1.b.

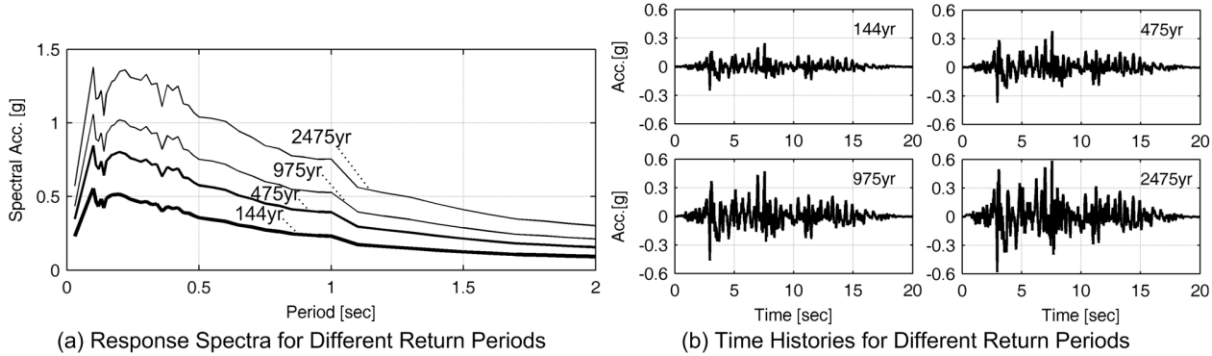


Figure 5.1. Earthquake Ground Motion Time Histories

### 5.2. Comparison of the Results from 2 and 3D Models

The transient analyses of the Cokal Dam were performed using the 2 and 3D models for the design earthquakes provided above. For the sake of brevity, the results provided in this section are limited to analyses for the 144 and 2475 year return period events. The comparison of the envelope of shear strains obtained from the 2 and 3D analyses is provided in Figure 5.2.a. at the maximum cross section of the dam. The distribution of the shear strains near the upstream and downstream faces appeared similar. However, it is observed that the 3D model yielded somewhat smaller shear strains towards the centre of the embankment. The comparison of displacement histories at the crest of the dam is provided in Figure 5.2.b. for the 2 and 3D analyses. The lateral displacements at the crest of the dam were obtained very similarly for both models.

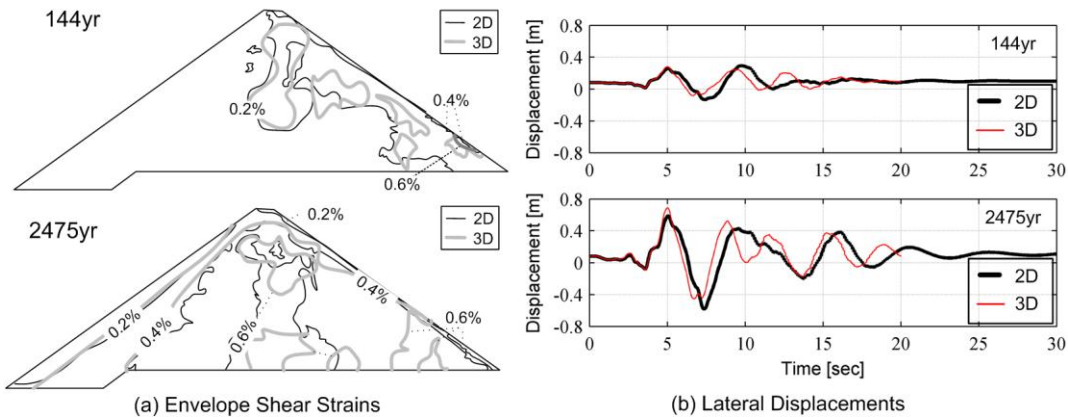
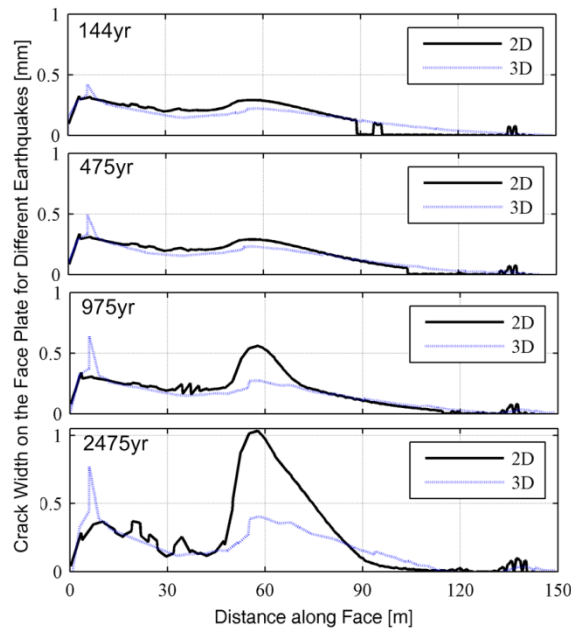


Figure 5.2. Comparison of 2 & 3D Fill Response for Different Earthquakes

The variation of the axial stress on the face plate serves as an indicator of the behavior of the face plate during the earthquake excitation. The tensile demand on the plate increases during earthquake

excitation. The state of the cracking on the face plate as a result of this increase in the tensile stresses is provided in Figure 5.3. For the 144 year return period event, the state of the cracking on the face plate was very similar for the 2 and 3D models. The cracking on the face plate spread as far as 120m away from the plinth base towards the crest of the dam. The cracking was uniformly distributed on the plate except for a concentration around the mid-height of the dam. For the event with a 475 year return period, a similar pattern was observed. However, for the stronger events, the results obtained from the 2 and 3D models were somewhat different, i.e. 1) the crackwidth predicted around the mid-height of the plate was much larger for the 2D model and 2) the largest crack was predicted at the bottom of the plate for the 3D model. While a growth in the width of the crack at the mid-height of the dam was also observed for the 3D model, this effect was not as prevalent as it was compared to the 2D analysis results.



**Figure 5.3.** Crack-width on the Face Plate-Different Earthquakes

### 5.3. Spatial Effects of the Earthquake Excitation on the Face Plate

The adverse effects of the earthquake loading on the face plate is perhaps displayed best by showing the distribution of the cracking on the plate for the range of considered ground motions (Figure 5.4.). The significant increase in the cracked area on the plate after the earthquake motion is evident for the 144 and 475 year return period events; however, the maximum crackwidth was not significantly affected from the earthquakes of these return periods. The 975 and 2475 year return period earthquakes were much more destructive on the face plate; cracks of 0.4-0.5mm width, observed only at the very bottom of the plate for the lower intensity events, spread towards the mid-height of the plate. Moreover, some zones of extensive damage were obtained; crackwidths as large as 5mm were obtained at one location for the 975 year return period event and at two locations for the 2475 year return period event. At these locations, the compressive strength of the concrete face plate was exceeded leading to the crushing of the face plate.

The time history of the compressive stress observed on the face plate is presented in Figure 5.5.a. in order to shed a light to this behavior. The time histories shown in this figure for the 144 and 2475 yr events correspond to the history of the compressive stress obtained parallel to the dam axis. These plots are provided for the location on the plate where the maximal compressive stress within the earthquake duration was observed. The maximum compressive stress for the 144 yr event was around 8 MPa obtained near the valley side, with the plate reverting to 6 MPa stress after the end of the earthquake shaking. On the other hand, the exceedance of the strength of the plate was observed for

the 2475 year return period event near the crest of the dam leading to the crushing of the plate. The crushing behaviour led to a permanent damage on the face plate; the vertical construction joint was opened to a significant degree after the damage.

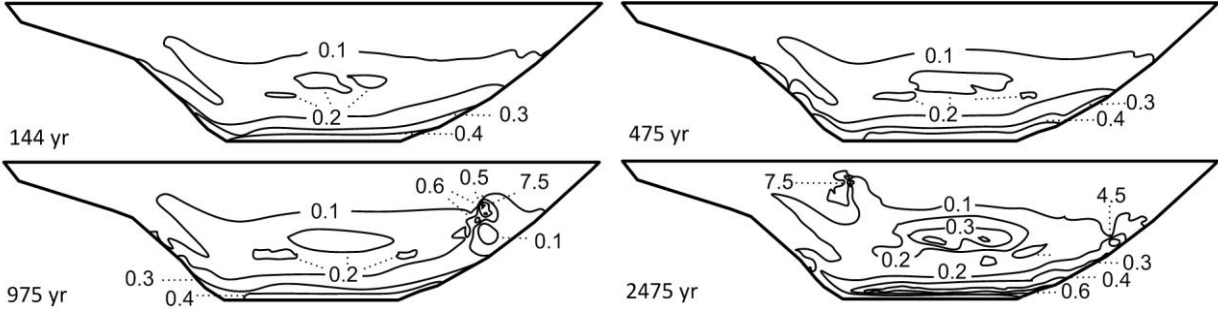


Figure 5.4. Contours of Crackwidth after Earthquakes with Different Return Periods (in mm’s)

The residual opening after the end of the earthquake motion is provided in Figure 5.5.b. Many of the joints appeared to have gone through a cycle of opening and closing during the ground motion, at the end of the earthquake motion, a small percentage of joints remained open; permanent openings were confined to the lower parts of these joints close to the valley sides. The residual values of openings at the vertical construction joints were significantly larger and much more dispersed for the earthquake with a 2475 year return period. As mentioned above, there were two locations at which the crushing of the face plate has led to some large openings (as large as 5cm) in the vertical construction joints.

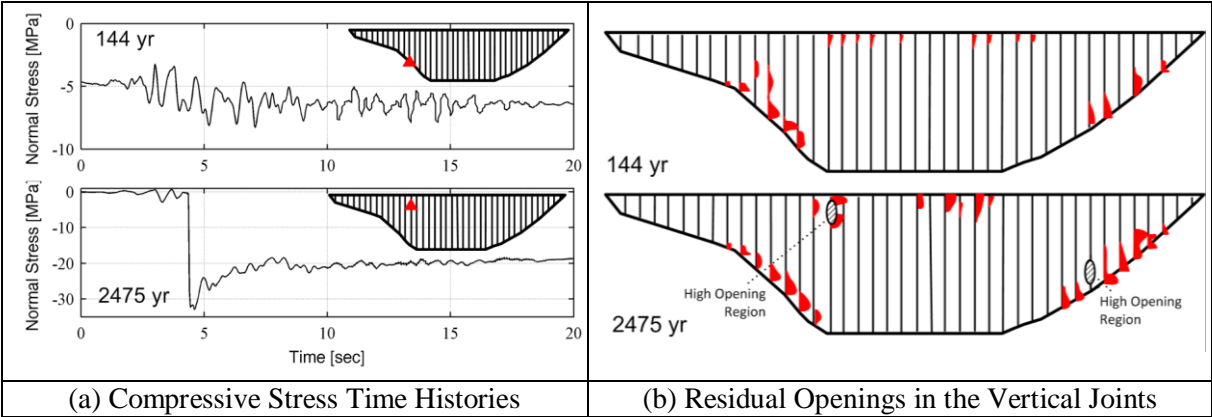


Figure 5.5. Comparison of Face Plate Response for the Earthquake Events with 144 and 2475 yr Return Periods

6. CONCLUSIONS

In this study, the performance of the face plate of a CFRD was investigated with a focus on crack development during the impounding and the earthquake loading. 2 and 3D modeling approaches for the modeling of cracking on the face plate of a CFRD were compared in order to determine the critical aspects of the behavior of the water retaining component of a CFRD. The following conclusions can be drawn based on the analysis results.

- Lateral cracking parallel to the main axis of the dam was observed to be the prevalent behavior of cracking on the face plate for the impounding stage. This cracking was spread on the face plate except for a large region at the center of the plate. Cracking parallel to the vertical construction joints was very limited, with significantly smaller crack widths concentrated to the valley sides at the base of the dam.
- The lateral cracking on the face plate increased considerably after the earthquake event even for a 144 yr earthquake. For the 2475 yr event, a major portion of the face plate was observed to be in a cracked state for both the 2 and 3D analyses. Most of these cracks appeared to be small in nature, i.e.

cracking at the base of the plate after the impounding spread higher on the plate after a strong ground motion.

- The maximum crackwidth predicted for the milder earthquake events (144 and 475 years return periods) are similar for the 2 and 3D analyses. On the other hand, for the 2475 year return period earthquake, a much larger crackwidth around the mid-height of the face plate was predicted in the 2D analysis compared to the 3D counterpart.
- The primary damage on the face plate was the crushing of the plate observed for the 975 and 2475 year return period events. The crushing of the plate in these events led to significantly large crackwidths on the vertical construction joints. Crushing was not observed for the earthquake events with 144 and 475 year return periods; the face plate performed satisfactorily.

## ACKNOWLEDGEMENTS

This study has been conducted with the funding provided by The Scientific and Technological Research Council of Turkey (TUBITAK) under the grant MAG108M491.

## REFERENCES

- ACI Committee 318.(2004). Building Code Requirements for Structural Concrete and Commentary 2005. *American Concrete Institute*.
- Arici, Y.(2011). Investigation of the cracking of CFRD face plates. *Comput Geotech.* 38, 905-916.
- Chen, S. S., Han, H.Q. (2009). Impact of the '5.12' Wenchuan earthquake on Zipingpu concrete face rockfill dam and its analysis. *Geomechanics and Geoengineering: An Int J.* **Vol IV.** S4-299-S4-306.
- Feenstra, P. H., Rots, J. G., Arnesen, A., Teigen, J. G., Høiset, K. V.(1998). A 3D constitutive model for concrete based on a co-rotational concept. In: B.B. R. de Borst et al., editors, EURO-C 1998, *Computer Modeling of Concrete Structures. Rotterdam: Balkema. The Netherlands.* p. 13-22.
- Gergely, P., Lutz, L. A.(1968). Maximum crack width in reinforced concrete flexural members. In: R.E. Philleo, editor. *Causes, mechanism and control of cracking in concrete, SP20, Detroit: American Concrete Institute.* p. 87-117.
- Groen, A. E.(1995). Elastoplastic modelling of sand using a conventional model. *Tech Rep 03.21.0.31.34/35, Delft University of Technology.*
- Johannesson, P. and Tohlang, S.L. (2007). Lessons learned from Mohale. *International Water Power and Dam Construction* [online]. Available from: <http://www.waterpowermagazine.com> [Accessed 29 March 2011].
- Pinto, N. L. (2007). S. A challenge of very high CFRD dams: Very high concrete face compressive stresses. *In the Proceedings of the 5<sup>th</sup> Int Conf on Dam Eng, Lisbon, Portugal.*
- Seed, H. B., Wong, R. T., Idriss, I. M., Tokimatsu, K.(1984). Moduli and Damping Factors for Dynamic Analysis of Cohesionless Soils. Rep No 84/14 . EERC, Berkeley, California.
- Sobrinho, J. A., Xavier, L. V., Albertoni, C., Correa, C., Fernandes, R. (2007). Performance and concrete repair at Campos Novos. *Hydropower Dams. Vol II.*
- TNO DIANA. (2008). User's Manual R. 9.3.
- Varadarajan, A., Sharma, K. G., Venkatachalam, K., Gupta, A. K.(2003). Testing and modeling two rockfill materials. *J Geotech Geoenv Eng.* 129:3, 206–218.
- Vermeer, P. A., De Borst, R.(1984). Non-associated plasticity for soils, concrete and rock. *Heron.* 29:3, 3-64.
- Zhang, G., Zhang, J. M.(2009). Numerical modelling of soil-structure interface of a concrete face rockfill dam. *Comput Geotech.* 36:5, 762–772.